Excited State Intramolecular Charge Transfer Suppressed Proton Transfer Process in 4-Diethylamino-2-Hydroxy-Benzaldehyde.

ARTICLE *in* THE JOURNAL OF PHYSICAL CHEMISTRY A · MAY 2013

Impact Factor: 2.69 · DOI: 10.1021/jp3120463 · Source: PubMed

3 AUTHORS, INCLUDING:

Sankar Jana
Tohoku University
33 PUBLICATIONS **350** CITATIONS

THE JOURNAL OF PHYSICAL CHEMISTRY A

Article

pubs.acs.org/JPCA

Excited State Intramolecular Charge Transfer Suppressed Proton Transfer Process in 4-(Diethylamino)-2-hydroxybenzaldehyde

Sankar Jana, Sasanka Dalapati, and Nikhil Guchhait*

Department of Chemistry, University of Calcutta, 92, A.P.C. Road, Kolkata-700009, India

Supporting Information

ABSTRACT: In this work, we report intramolecular charge transfer (ICT) suppressed excited state intramolecular proton transfer (ESIPT) process in 4-(diethylamino)-2-hydroxybenzaldehyde (DEAHB). Photophysical properties of DEAHB have been extensively studied in different solvents with varying pH, polarity, and hydrogen bonding capability of the solvent using steady state and time-resolved spectroscopy. To establish the competition between the ICT and ESIPT processes in DEAHB, we have synthesized and studied the photophysical properties of 4-(diethylamino)-2-methoxybenzaldehyde (DEAMB) molecule where only the charge transfer process has been observed. Recently, we have reported simple Schiff base molecules (*J. Phys. Chem. A* **2012**, *116*, 10948) formed by condensation of DEAHB and hydrazine (5-(diethylamino)-2-[(4-(diethylamino)benzylidene)hydrazonomethyl]phenol (DDBHP) and *N*,*N*′-bis(4-*N*,*N*-(diethylamino)salisalidene)hydrazine (DEASH)), where charge transfer is assisted by the proton transfer process. In the present case, the DEAHB molecule shows the reverse phenomenon; i.e., charge transfer is suppressed by the proton transfer process. Comparing the photophysical properties of DEAHB with DEAMB it is also found that ICT process in DEAHB is suppressed by the ESIPT process.

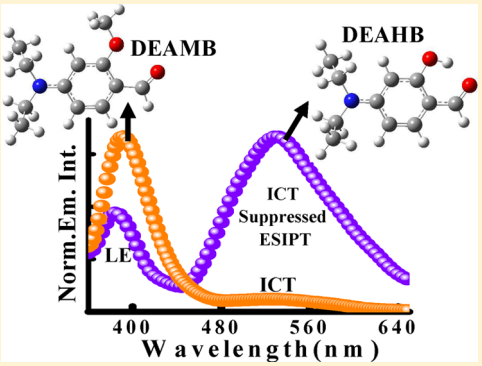

1. INTRODUCTION

The phenomenon of excited state intramolecular proton transfer (ESIPT) reaction has been extensively investigated over the past few decades due to their interesting photophysical and photochemical properties and their vast applications in the field of biochemistry, analytical chemistry, electrochromic modulation, perturbation of electronic state by variation of solvent polarity, laser dyes, molecular memory storage devices, fluorescent probes, polymer protectors, metabolic process of living systems, and so on.[1−5] On the other hand, for many years in the field of photochemistry and photobiology, intramolecular charge transfer (ICT) fluorescent probes containing donor and acceptor groups have found new avenues for applications such as pH[6] and ion detectors, in creation of new optoelectronic devices such as electroluminescence devices, solar cells and thin film transistors,[7−9] and chemical sensors[10,11] for free volume measurement in polymers and degree of water penetration into the surfactant aggregates, for the study of biomimetic environments for sensing the local polarity around the binding sites of biologically relevant systems like proteins,[12−14] in biological light harvesting processes such as photosynthesis, etc. From the aspect of photophysical properties it would be interesting when both the ESIPT and ICT are coupled in a single molecular system.[15−18]

The ESIPT was first observed by Weller in 1956[19] where four level transitions via enol and keto form in the ground and excited state was established. The types of systems studied for proton transfer reaction can be broadly classified into three categories. The first category comprises systems with proton donor and acceptor sites within the same molecule having cyclic intramolecular hydrogen bonded (IMHB) ring in the ground state, which facilitates proton transfer in the excited state.[20] Two others types are excited state double proton transfer and multiproton transfer systems.[21] The ICT process was first reported by Lippert et al.[22] in the benchmark molecule 4-(dimethylamino)benzonitrile (DMABN). Various models have been proposed to explain the observed dual fluorescence of DMABN and in similar types of molecules with donor−acceptor moieties attached to a chromophore. The twisted intramolecular charge transfer (TICT),[8] rehybridized intramolecular charge transfer (RICT),[23] wagging intramolecular charge transfer (WICT),[24] and planarized intramolecular charge transfer (PICT) model,[25] etc. are some of the most discussed among them. To date, it has been found that the TICT model is the most acceptable one for explaining dual emission in DMABN and its analogous systems. Recently, we have reported the ICT reaction and coupled ESIPT and ICT reaction in a number of interesting self-designed synthetic molecular systems.[6,8,26,27] The coupled ESIPT and ICT reactions were also reported by Kasha,[28] Chou,[29] Lim,[30] and Rodriguez-Prieto's groups[31] in some molecular systems. Till now, there is no report of a molecular system having both the ICT and ESIPT sites where ICT process is suppressed by ESIPT process. In recent time, we have reported simple Schiff

Received: December 7, 2012
Revised: May 1, 2013
Published: May 3, 2013

base molecules (DDBHP and DEASH) formed by condensation of DEAHB and hydrazine molecules, where charge transfer has been assisted by proton transfer process.[18] But there is no report where a molecule shows the reverse phenomenon, i.e., suppression of intramolecular charge transfer by intramolecular proton transfer process.

For establishing the ICT suppressed ESIPT process, we have elaborately examined the photophysical properties of the 4-*N*,*N*′-(diethylamino)-2-hydroxybenzaldehyde (DEAHB) molecule (Scheme 1) containing both the possibilities of ICT and ESIPT reactions. At the same time, we have also synthesized and studied the photophysical properties of 4-*N*,*N*′-(diethylamino)-2-methoxybenzaldehyde (Scheme 1) where only solvent polarity dependent excited state intramolecular charge transfer is expected. It is reported that the molecule DEAHB has been widely used for synthesis of antimicrobial drugs[32] as well as various metal complexes that have antimicrobial activity[33] and also acts as metalloenzymes. We are interested to explore whether ICT and ESIPT processes occur independently or there is any dependency in the DEAHB molecule. Here, the photophysical properties have been reported on the basis of X-ray crystal structure, steady state absorption, emission spectroscopy, quantum yield calculations, and time-resolved measurements. Calculation of radiative, nonradiative decay rate constant, and polarity dependent Stokes' shift help us to establish the occurrence of ICT suppressed ESIPT process in our DEAHB molecule.

Scheme 1. Optimized Structure of DEAHB and DEAMB Using the B3LYP Hybrid Functional and the 6-311++G(d,p) Basis Set in Gaussian 03

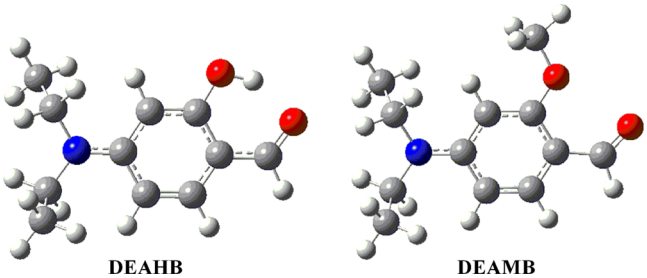

2. EXPERIMENTAL DETAILS

2.1. Materials. 4-*N*,*N*′-(Diethylamino)-2-hydroxybenzaldehyde was purchased from Aldrich Chemicals and used as received. Spectroscopic grade solvents were purchased from Spectrochem India Pvt. Ltd. and were used after proper distillation as needed. Details of all these solvents are given in the Supporting Information. Ethanol and sulfuric acid from E. Merck were used as received. Sodium hydroxide, phosphorous oxychloride ($POCl_3$) and diethyl(3-methoxyphenyl)amine were purchased from SRL India Pvt. Ltd. and Alkemi Co. Pvt. Ltd., respectively. Triple distilled water was used for the preparation of all aqueous solutions.

2.2. Steady State Spectral Measurements. All the spectral measurements were done at $\sim 10^{-5}$ to 10^{-6} M concentrations of solute to avoid aggregation and self-quenching. The steady state absorption spectra of DEAHB and DEAMB were recorded on Hitachi UV−vis U-3501 spectrophotometer. All the emission spectra were recorded on a Perkin-Elmer LS55 fluorescence spectrophotometer equipped with a 10 mm quartz cell and a thermostat bath.[34]

The fluorescence quantum yields of DEAHB and DEAMB in solvents having different polarity were measured relative to quinine sulfate in 0.1 (M) sulfuric acid (Φ_f = 0.57) as a secondary standard and calculated on the basis of the following equation.[8]

$$\Phi_f = \Phi_f^0 \frac{n^2 A^0 \int I_f(\lambda_f)\, d\lambda_f}{n_0^2 A \int I_f^0(\lambda_f)\, d\lambda_f} \quad (1)$$

where n_0 and n are the refractive index of the solvents, A^0 and A are the absorbances, Φ_f^0 and Φ_f are the fluorescence quantum yields, and the integrals denote the area of the fluorescence band for the standard and the sample, respectively.

2.3. Measurement of Time-Resolved Emission Spectra. Fluorescence lifetimes were measured from time-resolved intensity decay by the method of time-correlated single-photon counting (TCSPC) technique by FluoroCube-01-NL spectrometer (Horiba Jobin Yovon IBH Ltd.) using a nano LED light source at 340 nm, and the signals were collected at the magic angle (54.7°) polarization. The IRF of detector is (fwhm) 750 ps. DAS6 software was used to deconvolute the fluorescence decays. The relative contribution of each component was obtained from the biexponential fitting and finally expressed by the following equation.[35]

$$a_n = \frac{B_n}{\sum_{i=1}^{N} B_i} \quad (2)$$

B_i is the pre-exponential factor. The mean fluorescence lifetimes for the decay curves were calculated from the decay times and the relative contribution of the components using the following equation.

$$\langle \tau \rangle = \frac{\sum a_i \tau_i^2}{\sum a_i \tau_i} \quad (3)$$

τ_i and a_i are the fluorescence lifetime and its coefficient of the ith component, respectively.

The radiative and nonradiative rate constants have been calculated using the following equations[10]

$$k_r = \Phi_f / \langle \tau \rangle \quad (4)$$

$$1/\langle \tau \rangle = k_r + k_{nr} \quad (5)$$

where k_r, k_{nr}, $\langle \tau \rangle$, and Φ_f are the radiative, nonradiative rate constant, average fluorescence lifetime, and fluorescence quantum yield, respectively.

3. RESULTS AND DISCUSSION

3.1. Structure of DEAHB in a Single Crystal at 298 K Temperature. The presence of the ground state intra- or intermolecular hydrogen bond network in a molecular system plays a crucial role for ESIPT reaction. Structurally, the molecule DEAHB has the possible six-member intramolecular hydrogen bonding site capable for ESIPT reaction. It would be worthwhile to know the exact solid state structure of DEAHB regarding the existence of hydrogen bond or any other interactions within the crystal packing at the experimental temperature (298 K). The solid state structure obtained from the X-ray single crystal structural analysis is shown in Figure 1a−c, and the data collection strategy and the details of structure refinement are summarized in Table S1 (Supporting Information). Single crystal analysis revels that it forms a triclinic crystal pattern with *P*-1space group (Figure 1a). Figure

dx.doi.org/10.1021/jp3120463 | J. Phys. Chem. A 2013, 117, 4367−4376

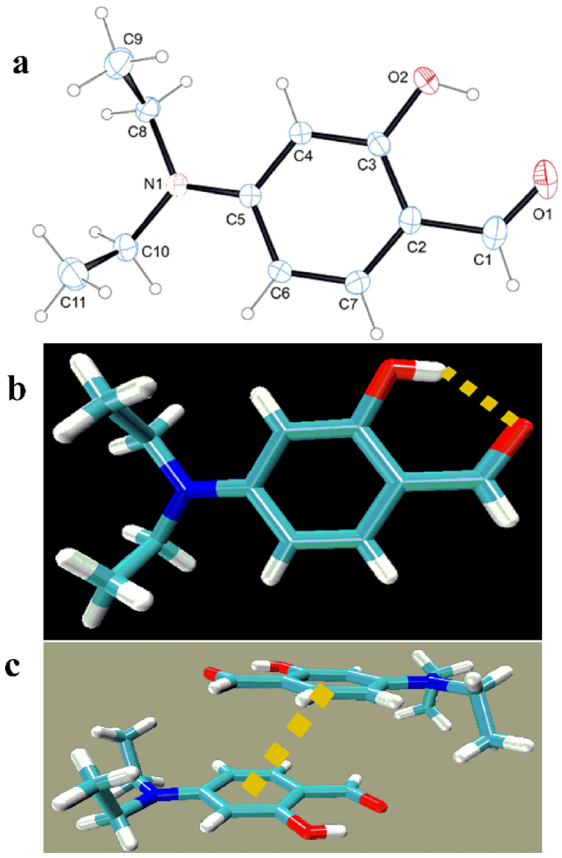

Figure 1. Single crystal structure of DEAHB: (a) ORTEP diagram (thermal ellipsoids set to 20% probability); (b) one intramolecular hydrogen bonding interaction with donor−acceptor distance 2.616 Å (the atom name and numbering are the same as that of the ORTEP diagram [atom colors: cyan, C; blue, N; red, O; gray, H]); (c) $\pi-\pi$ stacking interaction between two benzene rings.

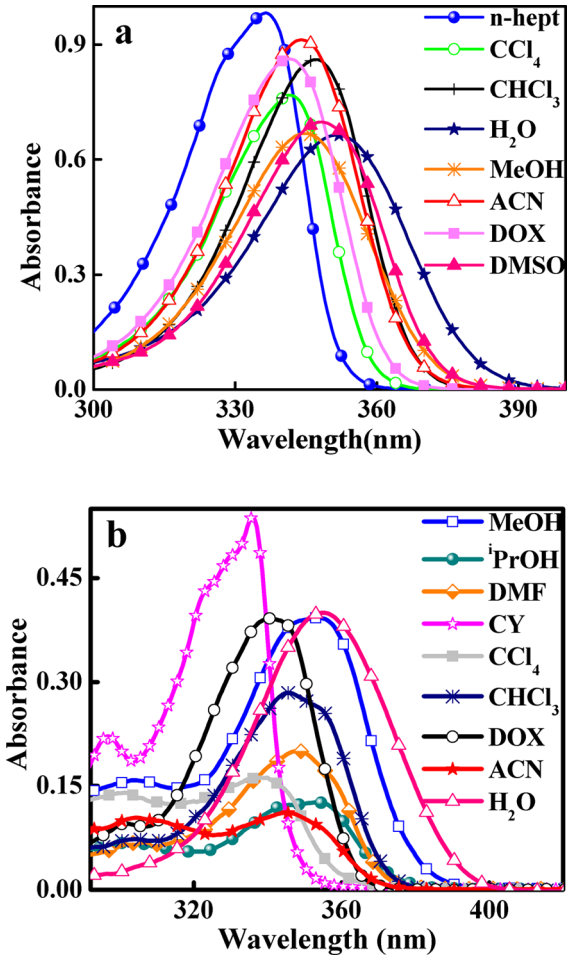

Figure 2. Absorption spectra of (a) DEAHB [conc 2.20 (*n*-hept), 1.72 (CCl_4), 1.80 ($CHCl_3$), 1.40 (H_2O), 1.42 (MeOH), 1.95 (ACN), 1.83 (DOX), 1.58 × 10^{-5} M (DMSO)] and (b) DEAMB [conc 1.30 (MeOH), 1.14 (^{i}PrOH), 1.23 (DMF), 1.49 (CY), 1.21 (CCl_4), 1.25 ($CHCl_3$), 1.34 (DOX), 1.09 (ACN), 1.31 × 10^{-5} M (H_2O)] at room temperature in different solvents with varying polarity and hydrogen bonding ability.

1b shows the presence of strong intramolecular hydrogen bonding interaction (O2−H2···O1) in the DEAHB molecule with O2···H2, H2···O1, and O2···O1 distances of 0.820, 1.890, and 2.616 Å, respectively, and the ∠O2−H2···O1 angle 147.0°. Therefore, the existence of intramolecular hydrogen bonding in the solid state crystal structure of DEAHB insists us to examine the possibility of the ESIPT reaction. Furthermore, each molecular unit of DEAHB is assembled through weak $\pi-\pi$ stacking interactions within the distance of 4.242 Å (distance between two centroids of benzene ring), where the perpendicular distance is 3.515 Å, α = 0°, and symmetry 2 − x, 1 − y, 1 − z (Figure 1c). As shown in Figure S1 (Supporting Information), a self-assembly of DEAHB through stacking interactions gives rise to 3D packing of DEAHB. In 2005, Vanco et al. reported the crystal structure of 4-*N*,*N*′-(diethylamino)-2-hydroxybenzaldehyde at very low temperature (120 K)[36] and showed an extra CH···π interaction, but from our crystal structure it is clear that with increase of temperature such type of CH···π interaction vanishes.

3.2. Absorption Spectra. The absorption spectra of DEAHB (~10^{-6} M) with variation of solvent polarity and hydrogen bonding capacity are shown in Figure 2a, and all the spectral band maxima are presented in Table 1. As seen in the figure, DEAHB shows broad absorption band at and around ~337 nm in nonpolar solvents, and ~345 nm in the case of polar protic and aprotic solvents. Comparing with the previously reported similar types of molecular systems,[26,27,37] the broad absorption band is assigned to both the $\pi \rightarrow \pi^*$ and n $\rightarrow \pi^*$ type of electronic transition within the wavelength range 330−355 nm. Red shifting of the absorption maxima in the case of a polar solvent is mainly due to different extents of ground and excited state solvent stabilization of DEAHB. It is found that the molecule possess high ground state dipole moment (ground state dipole moment is 6.59 D calculated at B3LYP functional and 6-311++G(d,p) basis set). On the other hand, DEAMB shows the absorption band within 335−355 nm wavelength range depending upon the polarity of solvents (Figure 2b). Although DEAMB shows similar band positions in the case of nonpolar and polar aprotic solvents, more red shifting of the absorption band (~355 nm) has been observed in hydrogen bonding solvents such as ^{i}PrOH, MeOH, EtOH, BuOH, H_2O, etc., which supports that hydrogen bonding solvents have much influence on the stabilization of the electronic states of DEAMB (calculated ground state dipole moment is 7.64 D at DFT level with B3LYP functional and 6-311++G(d,p) basis set) compared to that of DEAHB.

3.3. Steady State Emission Spectra. The steady state fluorescence spectra of DEAHB were recorded in different nonpolar, polar protic, and polar aprotic solvents by exciting at

dx.doi.org/10.1021/jp3120463 | J. Phys. Chem. A 2013, 117, 4367−4376

Table 1. Spectroscopic Parameters Obtained from Steady State Spectra of DEAHB and DEAMB in Different Solvents at Room Temperature[a]

	λ_{abs} (λ_{ex}^{max}) (nm)		λ_{em} (nm)		$\Delta\nu$ (cm^{-1})		$10^2 \times \Phi$	
solvent	DEAHB	DEAMB	DEAHB	DEAMB	DEAHB	DEAMB	DEAHB	DEAMB
n-hept	337 (333)		517		10331		0.275	
n-hex	336 (332)	336 (340)	524	392	10678	4251	0.412	41.9
MCH	337 (335)	336 (339)	522	393	10516	4316	0.248	16.2
CY	337 (334)	336 (340)	521	393	10480	4316	0.268	34.0
CCl_4	342 (337)	339 (342)	519	378	9972	3043	0.141	32.7
DCM	346 (348)	346 (349)	532	473, 388	10105	7760	0.047	15.3
$CHCl_3$	348 (350)	346 (350)	523	479, 389	9615	8024	0.082	18.4
THF	343 (344)		529		10251		0.074	
DOX	342 (340)	341 (348)	530	505, 383	10372	9523	0.081	0.8
DMF	347 (349)	348 (347)	532	512, 387	10021	9204	0.070	2.1
DMSO	349 (351)	349 (348)	531, 384	527, 388	9821	9677	0.102	2.2
ACN	345 (342)	345 (348)	530	518, 390	10118	9680	0.054	2.1
^{i}PrOH	344 (342)	354 (355)	528, 391	482, 384	10130	7501	0.040	2.5
BuOH	345 (348)	355 (357)	523, 385	385, 485	9865	7550	0.097	1.9
MeOH	345 (348)	354 (357)	523, 388	506, 391	9865	8485	0.069	0.7
EtOH	344 (347)	354 (355)	527	498, 388	10094	8168	0.056	1.0
H_2O	352 (354)	356 (354)	531, 401	415	9576	3993	0.035	0.2

[a] λ_{abs}, λ_{em}, $\Delta\nu$, and Φ are absorption, emission band position, Stokes shift, and fluorescence quantum yield, respectively. The error in quantum yield measurement is about ±6%.

the respective absorption maxima and are shown in Figure 3. All the steady state spectral data are presented in Table 1. It is

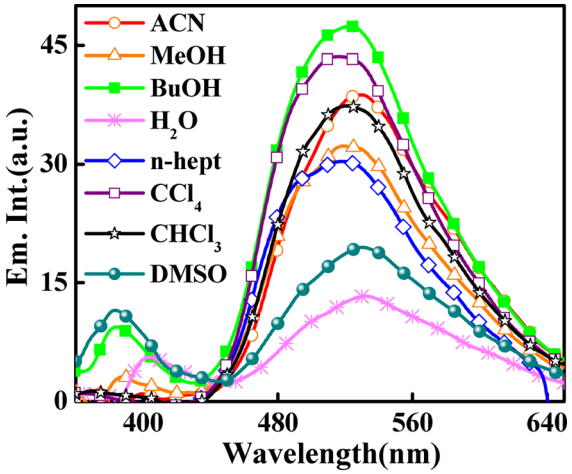

Figure 3. Emission profiles of DEAHB in different solvents [conc 0.10 (ACN), 0.09 (MeOH), 0.14 (BuOH), 0.03 (H_2O), 0.08 (*n*-hept), 0.12 (CCl_4), 0.11 ($CHCl_3$), 0.05 × 10^{-6} M (DMSO)] at room temperature.

seen that, in nonpolar solvents, DEAHB shows emission maxima at ~522 nm whereas it shows dual emission bands in a polar aprotic solvent like DMSO and hydrogen bonding solvents like ^{i}PrOH, BuOH, MeOH, etc. The higher energy emission band is observed at ~388 nm, and lower energy band, within the 523−531 nm wavelength range. Since DEAHB has both the charge transfer and proton transfer moieties, therefore the possibility of CT, PT, and local emission (LE) are expected in this molecule. In comparison with similar reported systems, the higher energy emission band at ~388 nm is assigned to the local emission.[26,27] But it is very difficult at this stage to assign the lower energy emission band to proton transfer/charge transfer bands or for both. For easy and safe assignment of the CT and PT emission bands, we have studied the emission properties of DEAMB, which is unable to show the PT emission band, because the transferable proton is replaced by methyl group. Under similar conditions, DEAMB shows one high energy emission band (~388 nm) in nonpolor solvents (Figure 4a) and dual emission in polar aprotic and polar protic solvents (Figure 4b), one at ~388 nm and another band within the 473−527 nm wavelength range depending upon the polarity of solvents. In comparison with the other reported systems in the literature, it is clear that the higher energy band of DEAMB is due to local emission and the lower energy band is nothing but the CT emission band.[6,26,27] These observations clearly insist us to assign the solvent polarity independent red-shifted emission band of DEAHB within 523−531 nm to the PT emission ($\pi \rightarrow \pi^*$ transition). Therefore, in comparison with the emission spectra of DEAHB and DEAMB, it is clear that, instead of PT and CT emission, DEAHB shows only polarity independent PT emission (due to intramolecular in nature) with very low intensity. The reason may be due to the fact that, after the charge transfer, the proton transfer process is favored by increasing the acceptor strength of the proton transfer moiety, which increases the possibility of proton transfer process.

3.4. Effect of pH on Steady State Absorption and Emission Spectra. To support the phenomena of ESIPT and/or ICT processes in DEAHB and the ICT process in DEAMB, steady state absorption and emission spectra were recorded in the presence of acid and base.[6,26] Addition of dilute sulfuric acid to the methanolic solution of DEAHB (Scheme 2a) produces a blue-shifted absorption band at ~280 nm with a simultaneous decrease in intensity of the original absorption band at ~345 nm through an isosbestic point at ~290 nm (Figure 5a). The blue-shifted band at ~280 nm is generated from the protonated species of DEAHB ($\pi \rightarrow \pi^*$ transition in substituted benzene system). The generation of the blue-shifted band is due to the protonation at the nitrogen center of the $-NEt_2$ group of DEAHB (Scheme 2b). The reason for blue shifting is due to resonance destabilization of the system after protonation.[6,8] In

dx.doi.org/10.1021/jp3120463 | J. Phys. Chem. A 2013, 117, 4367−4376

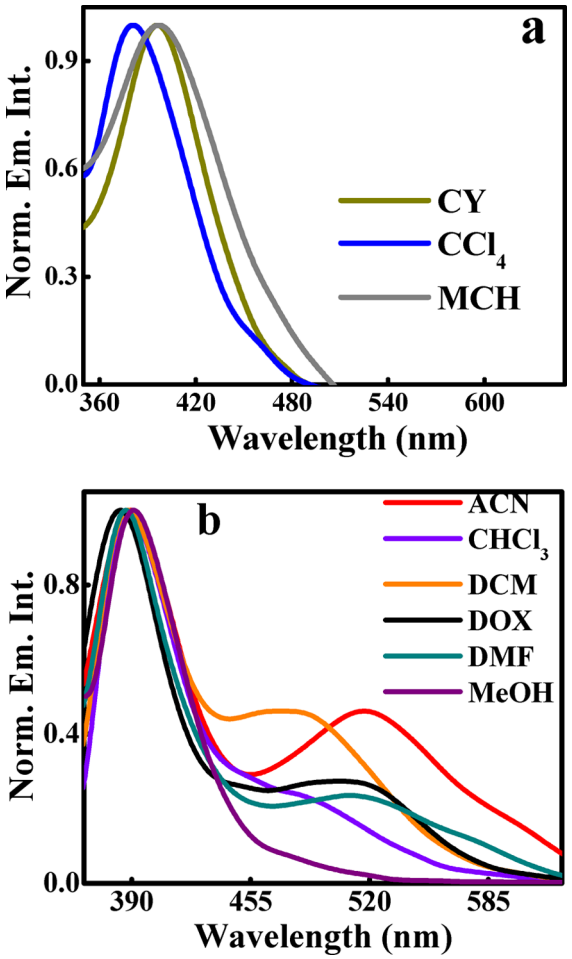

Figure 4. Normalized emission spectra of DEAMB in (a) nonpolar solvents [conc 0.12 (CCl_4), 0.15 (MCH), 0.13 × 10^{-6} M (CY)] and (b) polar protic and polar aprotic solvents [conc 0.18 (ACN), 0.74 ($CHCl_3$), 0.70 (DCM), 0.15 (DOX), 0.25 (MeOH), 0.23 × 10^{-6} M (DMF)] at 298 K.

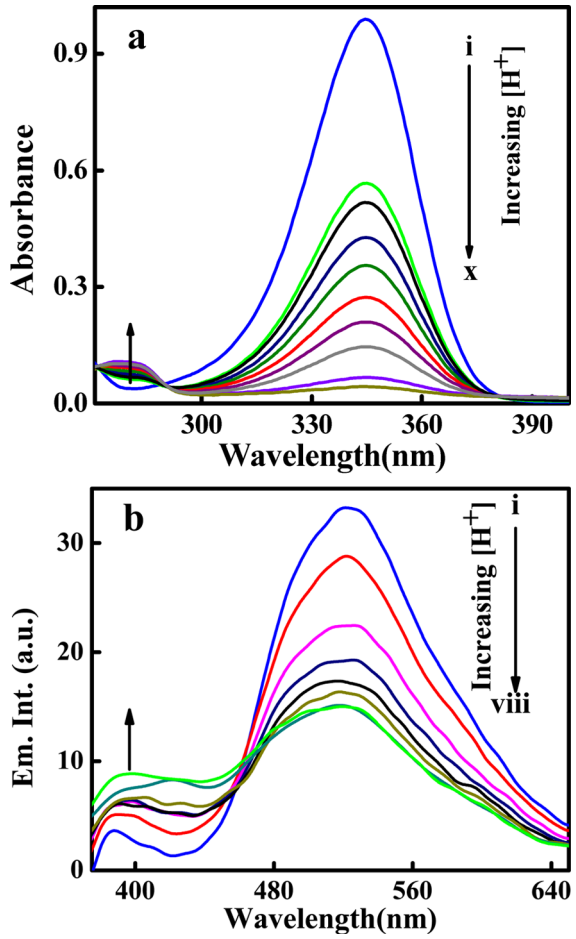

Figure 5. Effect of acid on steady state (a) absorption [DEAHB conc 1.85 × 10^{-5} M] (i → x: 0, 0.09, 0.8, 1.5, 5.4, 11.2, 18.4, 22.3, 27.8, 32.3 mM H_2SO_4) and (b) emission spectra [DEAHB conc 0.09 × 10^{-6} M] (i → viii: 0, 0.09, 0.5, 1.1, 1.6, 2.0, 2.4, 3.1) of DEAHB with increasing H_2SO_4 concentration in MeOH solvent.

Scheme 2. Probable Scheme for Protonation and Deprotonation of DEAHB by Diluted H_2SO_4 and Diluted NaOH, Respectively

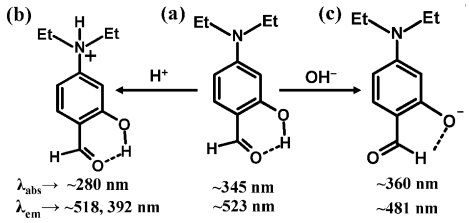

Scheme 3. Probable Protonated Scheme of DEAMB by Dilute H_2SO_4

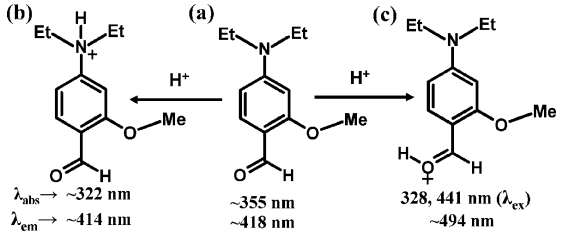

the case of the emission spectra (Figure 5b, λ_{ex} = 345 nm), with increasing sulfuric acid concentration, the original lower energy emission band at ~523 nm is slightly blue-shifted to ~518 nm with a decrease of emission intensity and at the same time a higher energy emission band was observed at ~392 nm through an isoemissive point at ~462 nm. The emission band at ~392 nm is thus assigned to the local emission of the protonated species of DEAHB and another band at ~518 nm is the proton transfer band of DEAHB[26] (Scheme 2b).

In the case of DEAMB (Scheme 3a), with increasing H_2SO_4 acid concentration to the aqueous solution, a blue-shifted absorption band at ~322 nm was observed at the expense of the original absorption band of DEAMB at ~355 nm (Figure 6a). Here also protonation can take place at the nitrogen center (Scheme 3b) and the blue shifting of the absorption maxima is due to the same reason as described before in the case of DEAHB. When emission spectra of DEAMB were recorded with increasing acid concentration (Figure 6b), a new emission band was observed with concomitant increase in emission intensity at ~494 nm. Additionally, a gradual decrease and slight blue shifting of the original emission band (from 418 to 414 nm) was observed. Here, protonation may be possible on both the N atom of the $-NEt_2$ group (Scheme 3b) and the O atom of the aldehyde group (Scheme 3c). Protonation at the N atom results in a blue shift of both the absorption and emission

dx.doi.org/10.1021/jp3120463 | J. Phys. Chem. A 2013, 117, 4367−4376

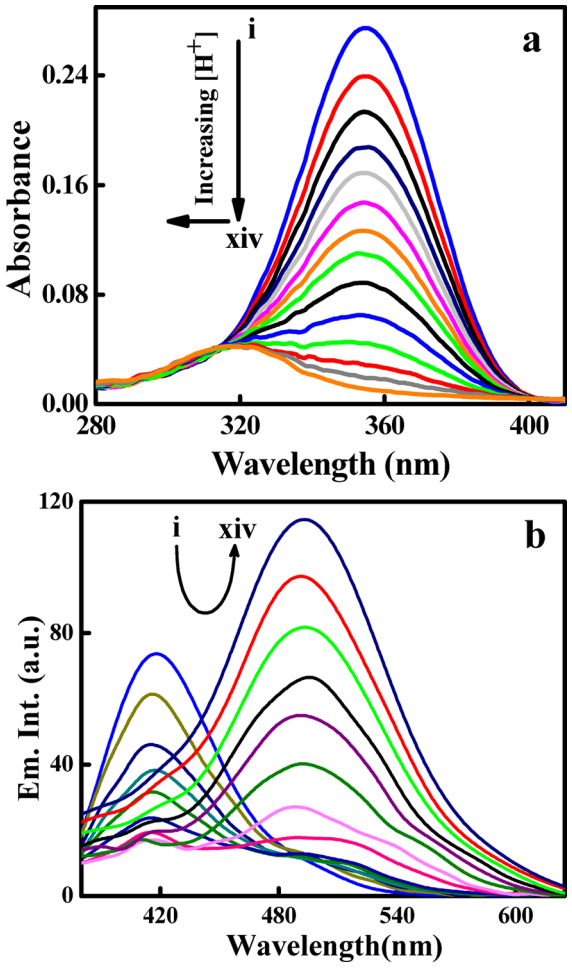

Figure 6. Effect of acid on steady state (a) absorption [DEAMB conc 0.98×10^{-5} M] (i → xiv: 0, 0.5, 1, 1.5, 2, 2.5, 3, 3.5, 4, 5, 6.5, 8, 9, 10.2 mM H_2SO_4) and (b) emission spectra [DEAMB conc 0.13×10^{-6} M] (i → xiv: 0, 0.5, 1, 1.5, 3, 6.5, 9.5, 11.5, 14, 15.5, 17, 20, 25, 30×10^2 mM H_2SO_4) of DEAMB with increasing concentration of H_2SO_4 in aqueous medium.

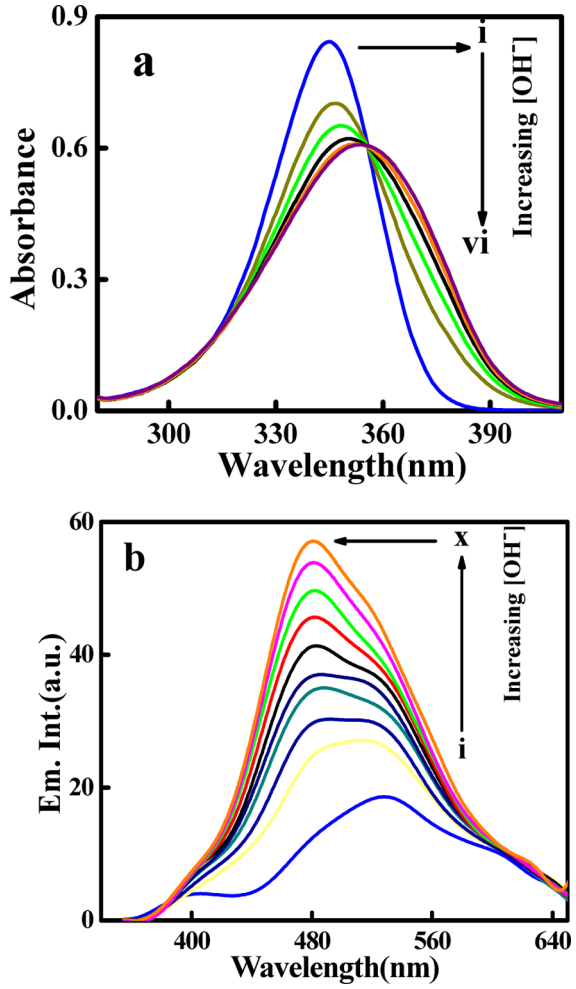

Figure 7. Effect of base on steady state (a) absorption [DEAHB conc 2.13×10^{-5} M] (i → vi: 0, 0.6, 1.2, 2.5, 3.3, 4 mM NaOH) and (b) emission spectra [DEAHB conc 0.06×10^{-6} M] (i → x: 0, 0.5, 0.9, 1.2, 2.6, 2.9, 3.3, 3.7, 4.5, 5.2 mM NaOH) of DEAHB with increasing NaOH concentration in MeOH solvent.

bands, as was discussed before for DEAHB.[8] At a high concentration of acid (>9.5 mM) protonation on the O atom of the aldehyde group may also be possible[27] due to the presence of an electron donating −OMe group at the ortho position of the acceptor aldehyde group. The aldehyde O atom becomes electron rich by electron donation from the −OMe group, and in this condition protonation occurs at the O atom.[27] As a result, the aldehyde group increases the charge acceptor ability by protonation at O atom and hence the CT process is favorable in the protonated form of DEAMB. Therefore, the large Stokes shifted emission band at 494 nm is the CT band of the protonated DEAMB molecule. We have also recorded the excitation spectra in the presence of acid by monitoring at the 494 nm emission maxima, which clearly shows two peaks: one at ∼328 nm (Figure S2, Supporting Information) resembles the absorption spectra of DEAMB in the presence of acid and another very weak band at 441 nm may be due to the excited state protonation at the O atom.

The effect of base on the absorption and emission properties of DEAHB has also been studied by the addition of NaOH solution to the methanolic solution of DEAHB. On gradual addition of base, the absorption spectra were found to be red-shifted with a decrease in absorbance value (Figure 7a). The newly generated red-shifted band at ∼360 nm originates from the anion of DEAHB, as shown in Scheme 2c. The red shifting of the absorption band may be due to resonance stabilization of the negative charge on the O atom (anion of DEAHB) via the acceptor aldehyde group or intramolecular hydrogen bonding interaction via the aldehyde hydrogen (Scheme 2c).[26] On the other hand, in the case of the emission spectra (λ_{ex} = 354 nm) enhancement of emission intensity with the blue shifting of the emission maxima from 531 to 481 nm was observed (Figure 7b). Here the newly generated blue-shifted emission band is nothing but the CT emission of the anion. The reason for blue shifting of the CT band of the anion compared to the red-shifted PT band of neutral DEAHB is due to destabilization of the excited state anion through the charge transfer process where there is a possibility of electronic repulsion between the negative charge of the anion and the charge transferred acceptor group after the ICT process.[26] The phenomenon of enhancement of emission intensity of the anion in the absence of the ESIPT process also supports the same phenomenon; i.e., in the presence of the ESIPT process the ICT process is suppressed (Scheme 4). On the other hand, DEAMB did not show any base effect in the absorption and emission spectra as it has no acidic hydrogen.

dx.doi.org/10.1021/jp3120463 | J. Phys. Chem. A 2013, 117, 4367−4376

Scheme 4. Probable Scheme of ESIPT and ICT processes in DEAHB

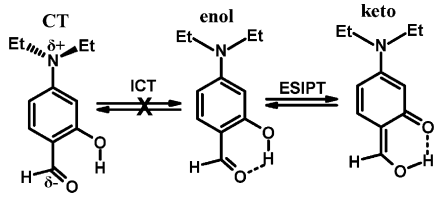

3.5. Excited State Polarity and Effect of Solvent. The high dipolar nature of the emissive species can be rationalized by solvatochromic shift of the CT emission band and by the change in the excited state dipole moment compared to the ground state. With increasing solvent polarity, the CT band of DEAMB shifts more to the red because the solvent dipoles orient themselves around the fluorophore to attain an energetically favorable arrangement, thereby stabilizing the polar CT state.[6,38] The excited state dipole moment has been calculated from the slope of the Lippert–Mataga plot (Stokes shift ($\Delta\nu$) vs solvent parameter $\Delta f(\varepsilon_r,n)$) as shown in Figure 8a. Following is the Lippert–Mataga relation[39]

$$\nu_a - \nu_f = \frac{(\mu^* - \mu)^2}{2\pi\varepsilon_0 hc\rho^3} \times f(\varepsilon_r,n)$$

where

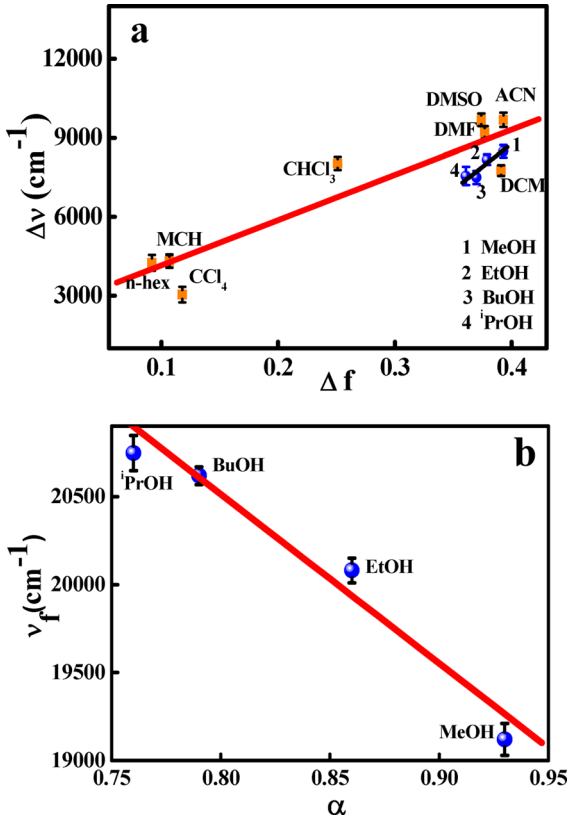

Figure 8. (a) Stokes shift ($\Delta\nu$) against solvent polarity parameter (Δf) (orange points for nonpolar and polar aprotic solvents; blue for polar protic solvents). (b) CT emission band maxima against hydrogen bonding parameter (α) for DEAMB. In each point, the black bar with a cap represents the error bar.

$$f(\varepsilon_r,n) = \left[\frac{\varepsilon_r - 1}{2\varepsilon_r + 1}\right] - \left[\frac{n^2 - 1}{2n^2 + 1}\right]$$

where ν_a, ν_f, ε_r, n are absorption and emission band positions (cm^{-1}), the dielectric constant, and the refractive index of the medium, respectively. The terms h, ε_0, c, ρ, μ, and μ^* are Planck's constant (6.626×10^{-34} J s), the permittivity of vacuum (8.85×10^{-12} C^2 N^{-1} m^{-2}), the velocity of light (3×10^8 m s^{-1}), the Onsagar cavity radius, and the ground and excited state dipole moments, respectively. It is found that the Lippert–Mataga plot for DEAMB shows linearity for nonpolar and polar aprotic solvents. The value of the Onsagar cavity radius (ρ) has been calculated to be 4.93 Å by a volume test of the optimized structure of DEAMB at the DFT level using the B3LYP functional and 6-311++G(d,p) basis set.[40] From the ratio of the slope obtained from the Lippert–Mataga plot and calculated values of ρ and μ, the excited state dipole moment has been calculated to be 20.55 D. The large difference in the dipole moment ($\Delta\mu$ = 12.91 D) from the ground state (μ = 7.64 D) to the excited state (μ^*=20.55 D) could only be possible by redistribution of charge in the excited state by the intramolecular charge transfer process from the $-NEt_2$ group to the acceptor aldehyde group upon photoexcitation of DEAMB.[8,22,41,42] It is impossible to calculate the excited state dipole moment of DEAHB by solvatochromic Stokes shift, because DEAHB did not show polarity dependent Stokes shifted emission band.

In the case of protic solvents, a deviation from linearity was observed in the Lippert–Mataga plot, which indicates that hydrogen bonding solvents have different types of influence on the nature of the CT state of DEAMB.[8] We have also plotted the position of the CT emission band maxima (ν_f, cm^{-1}) of DEAMB vs the hydrogen bonding parameter α[6,43] for protic solvents, as presented in Figure 8b. The linear nature of the plot supports that the red-shifted CT band in protic solvents is influenced by the intermolecular hydrogen bonding interaction. As seen in Figure 9a, the plot of Stokes' shift vs solvent polarity parameter $E_T(30)$[38] generates two straight lines with different slopes, one for the nonpolar, polar aprotic solvents and another for the polar protic solvents. This plot clearly indicates the presence of both the dipolar and hydrogen bonding interactions. A similar type of plot for DEAHB also generates two straight lines (Figure 9b): one for nonpolar, polar aprotic solvents and another for hydrogen bonding solvents. But the nature of the two lines is just opposite (negative slope), as is observed for DEAMB (positive slope). Here, with increasing $E_T(30)$ values, Stokes shift decreases, which means that DEAHB becomes less stabilized in hydrogen bonding solvents and more stabilized in nonpolar solvents.

3.6. Fluorescence Quantum Yield Measurement. The experimentally calculated fluorescence quantum yield values of DEAHB and DEAMB at room temperature with variation of solvent polarity and hydrogen bonding ability are provided in Table 1. The quantum yield values of DEAHB and DEAMB in nonpolar solvents are comparatively higher than in polar protic solvents. The low quantum yield value in polar protic solvents is mainly due to the presence of nonradiative decay channels, which are active via intermolecular hydrogen bonding interactions.[6,31] From the quantum yield data in Table 1, it can be interpreted that nonpolar solvents have different influence from that of the polar protic solvents on the ESIPT and ICT states. Comparison of fluorescence quantum yield between DEAHB and DEAMB (Table 1) reveals that the

dx.doi.org/10.1021/jp3120463 | J. Phys. Chem. A 2013, 117, 4367–4376

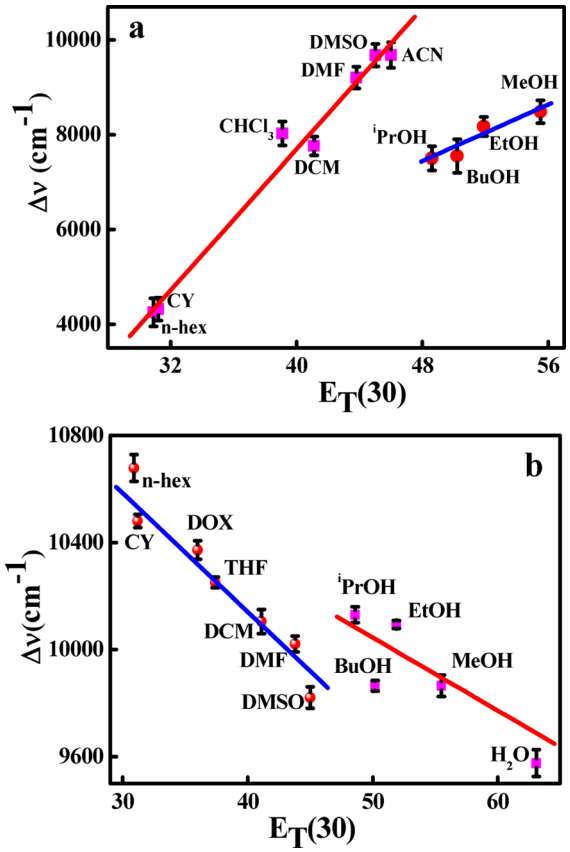

Figure 9. Plot of Stokes shift ($\Delta\nu$) against Reichardt solvent polarity parameter $E_T(30)$ for (a) DEAMB and (b) DEAHB. In each point, the black bar with cap represents the error bar.

quantum yields of DEAMB are almost 100 times more than that of DEAHB in different solvents. In DEAMB, only the ICT process is operative and results in very high quantum yield, but low quantum yield in case of DEAHB is due to the presence of the ESIPT process.[26,27,44]

3.7. Analysis of Fluorescence Lifetime. Fluorescence lifetimes were measured to investigate the excited state behavior of the molecules in different solvents. To know the exact origin of dual emission in DEAHB and DEAMB, we have performed time-resolved fluorescence measurement. All the decay curves have been well fitted by biexponential decay pattern with acceptable χ^2 values and all the time-resolved data are presented in Table 2. For all cases, there are two decay components, one component is ~99% and the other negligible component is only ~1%. In all solvents the major (~99%), fast decay component corresponds to the proton transfer (keto) form of DEAHB (Scheme 4).[26] Except for the ACN solvent, the average fluorescence lifetime of DEAHB in nonpolar and polar aprotic solvents are more compared to that of the polar protic solvents, where nonradiative decay channels are active. Radiative and nonradiative decay rate constant have been calculated and are presented in Table 2. As seen in Table 2, the nonradiative decay rate in hydrogen bonding polar solvents are higher compared to the nonpolar solvents. For the same reason the radiative decay rate constant shows the reverse order. This effect is also prominent in the measured quantum yield data, where higher fluorescence quantum yields are observed for nonpolar solvents and are lower in the case of polar protic solvents. In case of DEAMB, the contribution of two decay components are comparable in $CHCl_3$ where the faster component arises from the CT state and the slower component for the local excited state.[13,27] But in the case of polar aprotic and protic solvents, the faster and major component corresponds to the CT state. Overall, the average fluorescence lifetime of DEAMB is much higher than that of DEAHB.[26,27,30]

3.8. ICT Suppressed ESIPT Process. As seen in the emission spectra (Figure 4b, Table 1), DEAMB shows dual emission in polar aprotic and polar protic solvents. But, the emission spectra of DEAHB show only the proton transfer emission band within the 519−531 nm wavelength range (Figure 3, Table 1). Therefore, it can be concluded that the ICT process is suppressed by the presence of the ESIPT process in DEAHB (Scheme 4). Fluorescence lifetime values also support the same conclusion as that of the steady state emission data. The average fluorescence lifetime of DEAMB is within 0.9−1.4 ns (Table 2), which is in good agreement with similar types of charge transfer systems reported in the literature.[27,43,45] The CT process in the case of DEAHB is totally suppressed by the proton transfer process, and it shows the faster average fluorescence lifetime within the range ~0.2−0.5 ns.[46,47] If the charge transfer process is present, the

Table 2. Time-Resolved Components, Radiative (k_r) and Nonradiative (k_{nr}) Rate Constant of DEAHB and DEAMB in Different Solvents[a]

compound	solvent (λ_{em})	τ_1 (ns)	τ_2 (ns)	a_1	a_2	$\langle\tau\rangle$ (ns)	χ^2	$k_r \times 10^{-11}$ (s^{-1})	$k_{nr} \times 10^{-9}$ (s^{-1})
DEAHB	*n*-heptane (524)	0.290	0.937	0.986	0.013	0.317	1.16	0.867	3.140
	MCH (529)	0.289	0.899	0.983	0.016	0.319	1.18	0.778	3.123
	CCl_4 (528)	0.316	1.477	0.997	0.002	0.329	1.06	0.428	3.033
	$CHCl_3$ (529)	0.259	2.320	0.997	0.002	0.300	1.15	0.274	3.324
	DMF (532)	0.220	1.815	0.991	0.008	0.325	1.20	0.216	2.855
	DMSO (533)	0.233	4.493	0.997	0.002	0.424	1.29	0.240	2.113
	ACN (533)	0.180	0.796	0.992	0.007	0.199	1.12	0.270	5.005
	^{i}PrOH (513)	0.220	1.971	0.998	0.002	0.251	1.19	0.162	3.979
	BuOH (513)	0.229	1.754	0.997	0.002	0.253	1.14	0.383	3.941
	EtOH (513)	0.201	2.595	0.997	0.002	0.270	1.11	0.207	3.690
DEAMB	$CHCl_3$ (492)	0.532	1.687	0.481	0.518	1.425	1.06	12.905	0.572
	DMF (518)	0.543	5.612	0.981	0.018	1.387	1.17	1.513	0.705
	DMSO (524)	0.295	4.821	0.988	0.011	0.996	1.24	2.208	0.981
	ACN (522)	0.795	5.364	0.995	0.004	0.919	1.12	2.282	1.064

[a]Error in life time measurement is about ±5%.

dx.doi.org/10.1021/jp3120463 | J. Phys. Chem. A 2013, 117, 4367−4376

expected lifetime should be higher (>0.5 ns). Fluorescence quantum yield values (Table 1) are higher for the charge transfer process compared to the proton transfer process. Here, the low quantum yield values of DEAHB are only for proton transfer processes, which are present in higher percentage instead of combined charge transfer and proton transfer processes. The calculated Stokes shift (Table 1) also explains the same effect; i.e., only proton transfer occurs in higher percentage. Since the proton transfer process is intramolecular in nature, therefore it does not depend upon the polarity of the solvent, unlike the charge transfer process. In the case of DEAMB, the polarity dependent large Stokes shifted emission is observed whereas for DEAHB almost polarity independent Stokes shifted emission is observed. From all this evidence, it is clear that the charge transfer process is totally suppressed by the proton transfer process in DEAHB (Scheme 4). In contrast, the Schiff base molecules (DDBHP and DEASH) formed by condensation of DEAHB and hydrazine show charge transfer reaction which is assisted by the proton transfer process due to the change of acceptor group,[18] but the bare DEAHB molecule shows suppression of charge transfer by the proton transfer process.

4. CONCLUSIONS

In conclusion, we have reported the photophysical properties of DEAHB and DEAMB in different solvents with variation of pH, polarity, and hydrogen bonding ability. The solid state crystal structure of DEAHB at experimental temperature supports the possibility of a favorable ESIPT process within the cyclic six member hydrogen bonded system. DEAHB has different effect toward the hydrogen bonding solvents compared to that of the DEAMB. The comparison and elaborate photophysical study of DEAHB and DEAMB on the basis of the emission band position, Stokes shift, quantum yield, and lifetime data clearly conclude that the ICT process of DEAHB is suppressed by the ESIPT process. On the contrary, the Schiff base molecules (DDBHP, DEASH) derived from the benchmark molecule DEAHB and hydrazine show the reverse phenomenon, mainly due to the change of acceptor group.

■ ASSOCIATED CONTENT

Supporting Information

List of all the solvents, synthesis, and characterization of DEAMB, crystal packing 3D structure, excitation spectra of DEAMB in presence of acid, crystallographic parameters and refinement details. This information is available free of charge via the Internet at http://pubs.acs.org.

■ AUTHOR INFORMATION

Corresponding Author

*E-mail: nguchhait@yahoo.com. Tel: 91-33-23508386. Fax: 91-33-23519755.

Notes

The authors declare no competing financial interest.

■ ACKNOWLEDGMENTS

N.G. gratefully acknowledges the financial support received from Department of Science and Technology, India (Project no. SR/S1/PC-26/2008). S.J. and S.D. thank UGC for Fellowship.

■ REFERENCES

(1) Petek, H.; Zhao, J. Ultrafast Interfacial Proton-Coupled Electron Transfer. *Chem. Rev.* **2010**, *110*, 7082−7099.
(2) Hammes-Schiffer, S.; Stuchebrukhov, A. A. Theory of Coupled Electron and Proton Transfer Reactions. *Chem. Rev.* **2010**, *110*, 6939−6960.
(3) Lochbrunner, S.; Wurzer, A. J.; Riedle, E. Ultrafast Excited-State Proton Transfer and Subsequent Coherent Skeletal Motion of 2-(2[sup [prime]]-hydroxyphenyl)benzothiazole. *J. Chem. Phys.* **2000**, *112*, 10699−10702.
(4) Yahagi, T.; Fujii, A.; Ebata, T.; Mikami, N. Infrared Spectroscopy of the OH Stretching Vibrations of Jet-Cooled Salicylic Acid and Its Dimer in S_0 and S_1. *J. Phys. Chem. A* **2001**, *105*, 10673−10680.
(5) Mondal, S. K.; Sahu, K.; Ghosh, S.; Sen, P.; Bhattacharyya, K. Excited-State Proton Transfer from Pyranine to Acetate in γ-Cyclodextrin and Hydroxypropyl γ-Cyclodextrin. *J. Phys. Chem. A* **2006**, *110*, 13646−6339.
(6) Jana, S.; Ghosh, S.; Dalapati, S.; Kar, S.; Guchhait, N. Photoinduced Intramolecular Charge Transfer Phenomena in 5-(4-dimethylamino-phenyl)-penta-2,4-dienoic acid. *Spectrochim. Acta, Part A* **2011**, *78*, 463−468.
(7) He, C.; He, Q.; He, Y.; Li, Y.; Bai, F.; Yang, C.; Ding, Y.; Wang, L.; Ye, J. Organic Solar Cells Based on the Spin-Coated Blend Films of TPA-th-TPA and PCBM. *Sol. Energy Mater. Sol. Cells* **2006**, *90*, 1815−1827.
(8) Jana, S.; Dalapati, S.; Ghosh, S.; Kar, S.; Guchhait, N. Excited State Charge Transfer Reaction with Dual Emission from 5-(4-dimethylamino-phenyl)-penta-2,4-dienenitrile: Spectral Measurement and Theoretical Density Functional Theory Calculation. *J. Mol. Struct.* **2011**, *998*, 136−143.
(9) Kaletaş, B. K.; Mandl, C.; van der Zwan, G.; Fanti, M.; Zerbetto, F.; De Cola, L.; König, B.; Williams, R. M. Unexpected Photophysical Properties of Symmetric Indolylmaleimide Derivatives. *J. Phys. Chem. A* **2005**, *109*, 6440−6449.
(10) Jana, S.; Dalapati, S.; Alam, M. A.; Guchhait, N. Fluorescent Chemosensor for Zn(II) Ion by Ratiometric Displacement of Cd(II) Ion: A Spectroscopic Study and DFT Calculation. *J. Photochem. Photobiol. A* **2012**, *238*, 7−15.
(11) Jana, S.; Dalapati, S.; Alam, M. A.; Guchhait, N. Spectroscopic, Colorimetric and Theoretical Investigation of Salicylidene Hydrazine Based Reduced Schiff Base and its Application Towards Biologically Important Anions. *Spectrochim. Acta, Part A* **2012**, *92*, 131−136.
(12) Ding, F.; Huang, J.; Lin, J.; Li, Z.; Liu, F.; Jiang, Z.; Sun, Y. A Study of the Binding of C.I. Mordant Red 3 with Bovine Serum Albumin Using Fluorescence Spectroscopy. *Dyes Pigm.* **2009**, *82*, 65−70.
(13) Jana, S.; Dalapati, S.; Ghosh, S.; Guchhait, N. Potential Charge Transfer Probe Induced Conformational Changes of Model Plasma Protein Human Serum Albumin: Spectroscopic, Molecular Docking and Molecular Dynamics Simulation Study. *Biopolymers* **2012**, *97*, 766−777.
(14) Jana, S.; Ghosh, S.; Dalapati, S.; Guchhait, N. Exploring Structural Change of Protein Bovine Serum Albumin by External Perturbation Using Extrinsic Fluorescence Probe: Spectroscopic Measurement, Molecular Docking and Molecular Dynamics Simulation. *Photochem. Photobiol. Sci.* **2012**, *11*, 323−332.
(15) Sytnik, A.; Gormin, D.; Kasha, M. Interplay between Excited-State Intramolecular Proton Transfer and Charge Transfer in Flavonols and Their Use as Protein-Binding-Site Fluorescence Probes. *Proc. Natl. Acad. Sci.* **1994**, *91*, 11968−11972.
(16) Martín, C.; Gil, M.; Cohen, B.; Douhal, A. Ultrafast Photodynamics of Drugs in Nanocavities: Cyclodextrins and Human Serum Albumin Protein. *Langmuir* **2012**, *28*, 6746−6759.
(17) Kwon, J. E.; Lee, S.; You, Y.; Baek, K.-H.; Ohkubo, K.; Cho, J.; Fukuzumi, S.; Shin, I.; Park, S. Y.; Nam, W. Fluorescent Zinc Sensor with Minimized Proton-Induced Interferences: Photophysical Mechanism for Fluorescence Turn-On Response and Detection of Endogenous Free Zinc Ions. *Inorg. Chem.* **2012**, *51*, 8760−8774.

(18) Jana, S.; Dalapati, S.; Guchhait, N. Proton Transfer Assisted Charge Transfer Phenomena in Photochromic Schiff Bases and Effect of $-NEt_2$ Groups to the Anil Schiff Bases. *J. Phys. Chem. A* **2012**, *116*, 10948−10958.
(19) Beens, H.; Grellmann, K. H.; Gurr, M.; Weller, A. H. Effect of Solvent and Temperature on Proton Transfer Reactions of Excited Molecules. *Discuss. Faraday Soc.* **1965**, *39*, 183−193.
(20) Yu, W.-S.; Cheng, C.-C.; Cheng, Y.-M.; Wu, P.-C.; Song, Y.-H.; Chi, Y.; Chou, P.-T. Excited-State Intramolecular Proton Transfer in Five-Membered Hydrogen-Bonding Systems: 2-Pyridyl Pyrazoles. *J. Am. Chem. Soc.* **2003**, *125*, 10800−10801.
(21) Klerk, J. S. d.; Bader, A. N.; Zapotoczny, S.; Sterzel, M.; Pilch, M.; Danel, A.; Gooijer, C.; Ariese, F. Excited-State Double Proton Transfer in 1H-Pyrazolo[3,4-b]quinoline Dimers. *J. Phys. Chem. A* **2009**, *113*, 5273−5279.
(22) Lippert, E.; Luder, W.; Boos, H. *Advances in Molecular Spectroscopy; European Conference on Molecular Spectroscopy, Bologna, Italy, 1959* **1962**, 443−457.
(23) Sobolewski, A. L.; Domcke, W. Promotion of Intramolecular Charge Transfer in Dimethylamino Derivatives: Twisting Versus Acceptor-Group Rehybridization. *Chem. Phys. Lett.* **1996**, *259*, 119−127.
(24) Gorse, A.-D.; Pesquer, M. Intramolecular Charge Transfer Excited State Relaxation Processes in Para-Substituted N,N-Dimethylaniline: A Theoretical Study Including Solvent Effects. *J. Phys. Chem.* **1995**, *99*, 4039−4049.
(25) Zachariasse, K. A.; Druzhinin, S. I.; Bosch, W.; Machinek, R. Intramolecular Charge Transfer with the Planarized 4-Aminobenzonitrile 1-tert-Butyl-6-cyano-1,2,3,4-tetrahydroquinoline (NTC6). *J. Am. Chem. Soc.* **2004**, *126*, 1705−1715.
(26) Mahanta, S.; Singh, R. B.; Kar, S.; Guchhait, N. Evidence of Coupled Photoinduced Proton Transfer and Intramolecular Charge Transfer Reaction in para-N,N-Dimethylamino Orthohydroxy Benzaldehyde: Spectroscopic and Theoretical Studies. *Chem. Phys.* **2008**, *354*, 118−129.
(27) Samanta, A.; Paul, B. K.; Mahanta, S.; Singh, R. B.; Kar, S.; Guchhait, N. Evidence of Acid Mediated Enhancement of Photoinduced Charge Transfer Reaction in 2-methoxy-4-(N,N-dimethylamino)benzaldehyde: Spectroscopic and Quantum Chemical Study. *J. Photochem. Photobiol. A* **2010**, *212*, 95−104.
(28) Kasha, M. Proton-Transfer Spectroscopy. Perturbation of The Tautomerization Potential. *J. Chem. Soc., Faraday Trans.* **1986**, *82*, 2379−2392.
(29) Chou, P.-T.; Yu, W.-S.; Cheng, Y.-M.; Pu, S.-C.; Yu, Y.-C.; Lin, Y.-C.; Huang; Chen, C.-T. Solvent-Polarity Tuning Excited-State Charge Coupled Proton-Transfer Reaction in p-N,N-Ditolylaminosalicylaldehydes. *J. Phys. Chem. A* **2004**, *108*, 6487−6498.
(30) Zgierski, M. Z.; Fujiwara, T.; Lim, E. C. Coupled Electron and Proton Transfer Processes in 4-Dimethylamino-2-hydroxy-benzaldehyde. *J. Phys. Chem. A* **2011**, *115*, 10009−10017.
(31) Brenlla, A.; Rodríguez-Prieto, F.; Mosquera, M.; Ríos, M. A.; Ríos Rodríguez, M. C. Solvent-Modulated Ground-State Rotamerism and Tautomerism and Excited-State Proton-Transfer Processes in o-Hydroxynaphthylbenzimidazoles. *J. Phys. Chem. A* **2008**, *113*, 56−67.
(32) Padalkar, V.; Tathe, A.; Gupta, V.; Patil, V.; Phatangare, K.; Sekar, N. Synthesis and Photo-Physical Characteristics of ESIPT Inspired 2-Substituted Benzimidazole, Benzoxazole and Benzothiazole Fluorescent Derivatives. *J. Fluoresc.* **2012**, *22*, 311−322.
(33) N. Bessy, R.; R. Prathapachandra, K.; Suresh, E. Synthesis, Spectroscopic Characterization and Crystal Structure of Mixed Ligand Ni(II) Complex of N-4-Diethylaminosalicylidine-N-4-nitrobenzoyl Hydrazone and 4-Picoline. *Struct. Chem.* **2006**, *17*, 201−208.
(34) Jana, S.; Dalapati, S.; Ghosh, S.; Guchhait, N. Study of Microheterogeneous Environment of Protein Human Serum Albumin by an Extrinsic Fluorescent Reporter: A Spectroscopic Study in Combination with Molecular Docking and Molecular Dynamics Simulation. *J. Photochem. Photobiol. B* **2012**, *112*, 48−58.
(35) Jana, S.; Dalapati, S.; Ghosh, S.; Guchhait, N. Binding Interaction between Plasma Protein Bovine Serum Albumin and Flexible Charge Transfer Fluorophore: A Spectroscopic Study in Combination with Molecular Docking and Molecular Dynamics Simulation. *J. Photochem. Photobiol. A* **2012**, *231*, 19−27.
(36) Vanco, J.; Marek, J.; Svajlenova, O. 4-(Diethylamino)-salicylaldehyde. *Acta Crystallogr., Sect. E: Struct, Rep. Online* **2005**, *61*, 4209−4211.
(37) Chou, P.-T.; Wu, G.-R.; Wei, C.-Y.; Shiao, M.-Y.; Liu, Y.-I. Excited-State Double Proton Transfer in 3-Formyl-7-azaindole: Role of the $n\pi^*$ State in Proton-Transfer Dynamics. *J. Phys. Chem. A* **2000**, *104*, 8863−8871.
(38) Reichardt, C. Solvatochromic Dyes as Solvent Polarity Indicators. *Chem. Rev.* **1994**, *94*, 2319−2358.
(39) Mataga, N.; Chosrowjan, H.; Taniguchi, S. Ultrafast Charge Transfer in Excited Electronic Etates and Investigations into Fundamental Problems of Exciplex Chemistry: Our Early Studies and Recent Developments. *J. Photochem. Photobiol. C* **2005**, *6*, 37−79.
(40) Frisch, M. J.; Trucks, G. W.; Schlegel, H. B.; Scuseria, G. E.; Robb, M. A.; Cheeseman, J. R.; Montgomery, J. A.; Vreven, T.; Kudin, K. N.; Burant, J. C. et al. *Gaussian 03*, Revision C.02; Gaussian, Inc.: Pittsburgh, PA, 2003.
(41) Kawski, A.; Kukliński, B.; Bojarski, P. Excited State Dipole Moments of 4-(Dimethylamino)benzaldehyde. *Chem. Phys. Lett.* **2007**, *448*, 208−212.
(42) Atsbeha, T.; Mohammed, A.; Redi-Abshiro, M. Excitation Wavelength Dependence of Dual Fluorescence of DMABN in Polar Solvents. *J. Fluoresc.* **2010**, *20*, 1241−1248.
(43) Grabowski, Z. R.; Rotkiewicz, K.; Rettig, W. Structural Changes Accompanying Intramolecular Electron Transfer: Focus on Twisted Intramolecular Charge-Transfer States and Structures. *Chem. Rev.* **2003**, *103*, 3899−4032.
(44) Paul, B. K.; Samanta, A.; Guchhait, N. Deciphering the Photophysics of 5-Chlorosalicylic Acid: Evidence for Excited-State Intramolecular Proton Transfer. *Photochem. Photobiol. Sci.* **2010**, *9*, 57−67.
(45) Grabowski, Z. R.; Rotkiewicz, K.; Siemiarczuk, A. Dual Fluorescence of Donor-Acceptor Molecules and the Twisted Intramolecular Charge Transfer (TICT) States. *J. Lumin.* **1979**, *18−19*, 420−424.
(46) Stock, K.; Bizjak, T.; Lochbrunner, S. Proton Transfer and Internal Conversion of o-hydroxybenzaldehyde: Coherent Versus Statistical Excited-State Dynamics. *Chem. Phys. Lett.* **2002**, *354*, 409−416.
(47) Samanta, A.; Paul, B. K.; Kar, S.; Guchhait, N. Excited State Lactim to Lactam Type Tautomerization Reaction in 5-(4-Fluorophenyl)-2-hydroxypyridine: Spectroscopic Study and Quantum Chemical Calculation. *J. Fluoresc.* **2011**, *21*, 95−104.